SUPPLEMENTARY INFORMAION

Mutant lamins cause nuclear envelope rupture and DNA damage in skeletal muscle cells

Ashley J. Earle[1,*], Tyler J. Kirby[1,*], Gregory R. Fedorchak[1,*], Philipp Isermann[1], Jineet Patel[1], Sushruta Iruvanti[1], Steven A. Moore[2], Gisèle Bonne[3], Lori L. Wallrath[4], and Jan Lammerding[1,#]

[1] Meinig School of Biomedical Engineering & Weill Institute for Cell and Molecular Biology, Cornell University, Ithaca, NY, USA

[2] Department of Pathology, Carver College of Medicine, University of Iowa, Iowa City, IA USA

[3] Sorbonne Université, Inserm UMRS 974, Center of Research in Myology, Association Institute of Myology, Paris, France

[4] Department of Biochemistry, Carver College of Medicine, University of Iowa, Iowa City, IA, USA

[*] These authors contributed equally

The Supplementary Information contains Supplementary Figures, Tables, Movies, and References.

SUPPLEMENTARY FIGURES

Supp Fig. 1

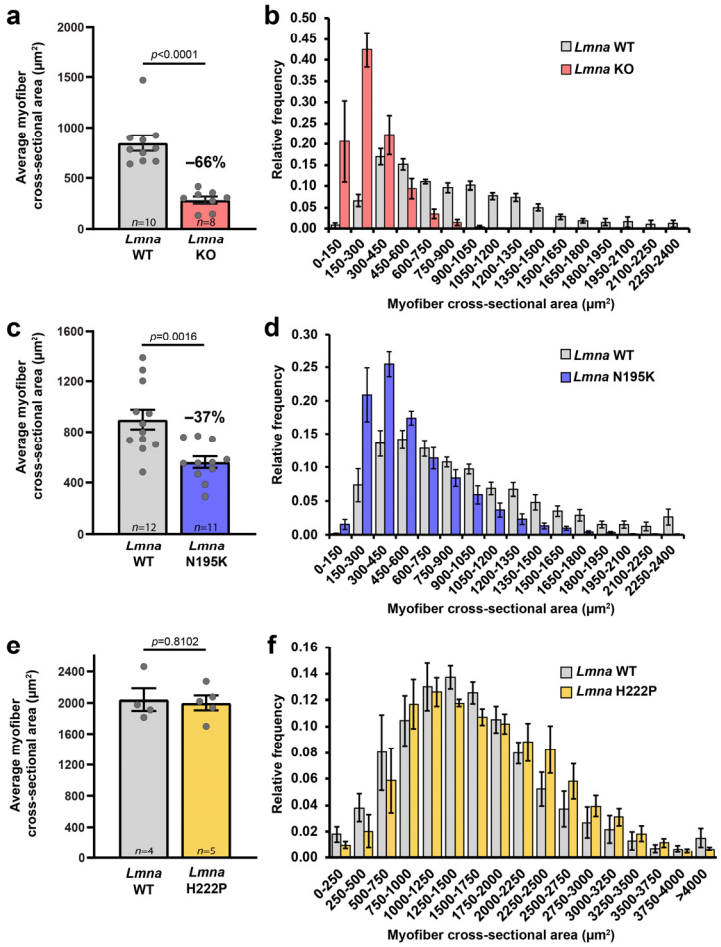

Supplementary Figure 1. ***Lmna*** **display varying degrees of muscular dystrophy**. (**a**) Quantification of the average myofiber cross-sectional area of *Lmna* WT and *Lmna* KO mice. Significance determined by two-tailed student's *t*-test. *n* indicates the number of mice per genotype. The percentage indicates the change relative to wild-type littermates. (**b**) Relative frequency of myofiber cross-sectional area in *Lmna* WT and *Lmna* KO mice, corresponding to the data from panel a. (**c**) Quantification of the average myofiber cross-sectional area of *Lmna* WT and *Lmna* N195K mice. Significance determined by two-tailed student's *t*-test. *n* indicates the number of mice per genotype. The percentage indicates the change relative to wild-type littermates. (**d**) Relative frequency of myofiber cross-sectional area in *Lmna* WT and *Lmna* N195K mice, corresponding to the data from panel c. (**e**) Quantification of the average myofiber cross-sectional area of *Lmna* WT and *Lmna* H222P mice. Significance determined by two-tailed student's *t*-test. *n* indicates the number of mice per genotype. (**f**) Relative frequency of myofiber cross-sectional area in *Lmna* WT and *Lmna* H222P mice, corresponding to the data in panel e. All bar plots show mean value ± standard error of the mean.

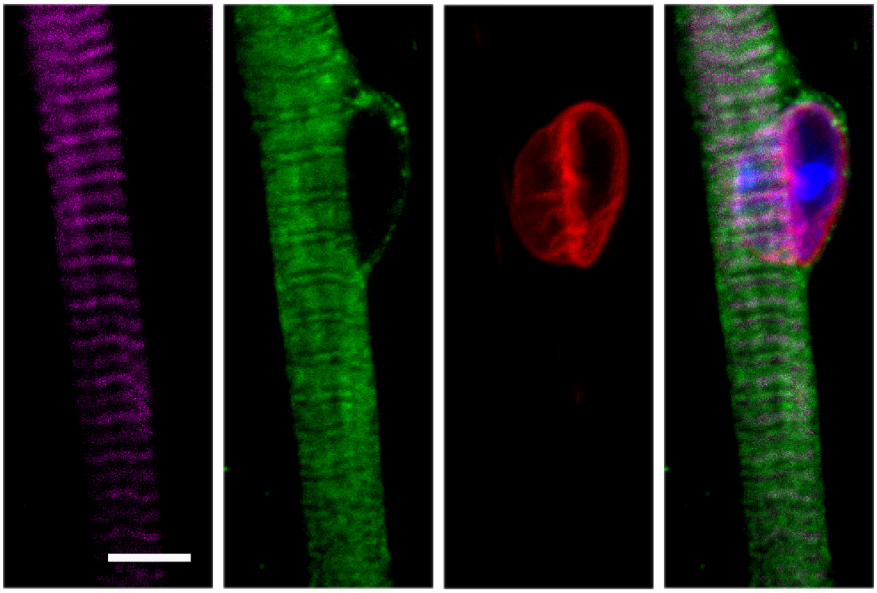

Supplementary Figure 2. ***In vitro*** **differentiation results in mature myofibers**. Representative image of a striated myofiber containing a peripheral nucleus at day 10 of differentiation. Scale bar: 5 µm. Image reflects results from experiments repeated three times with similar results.

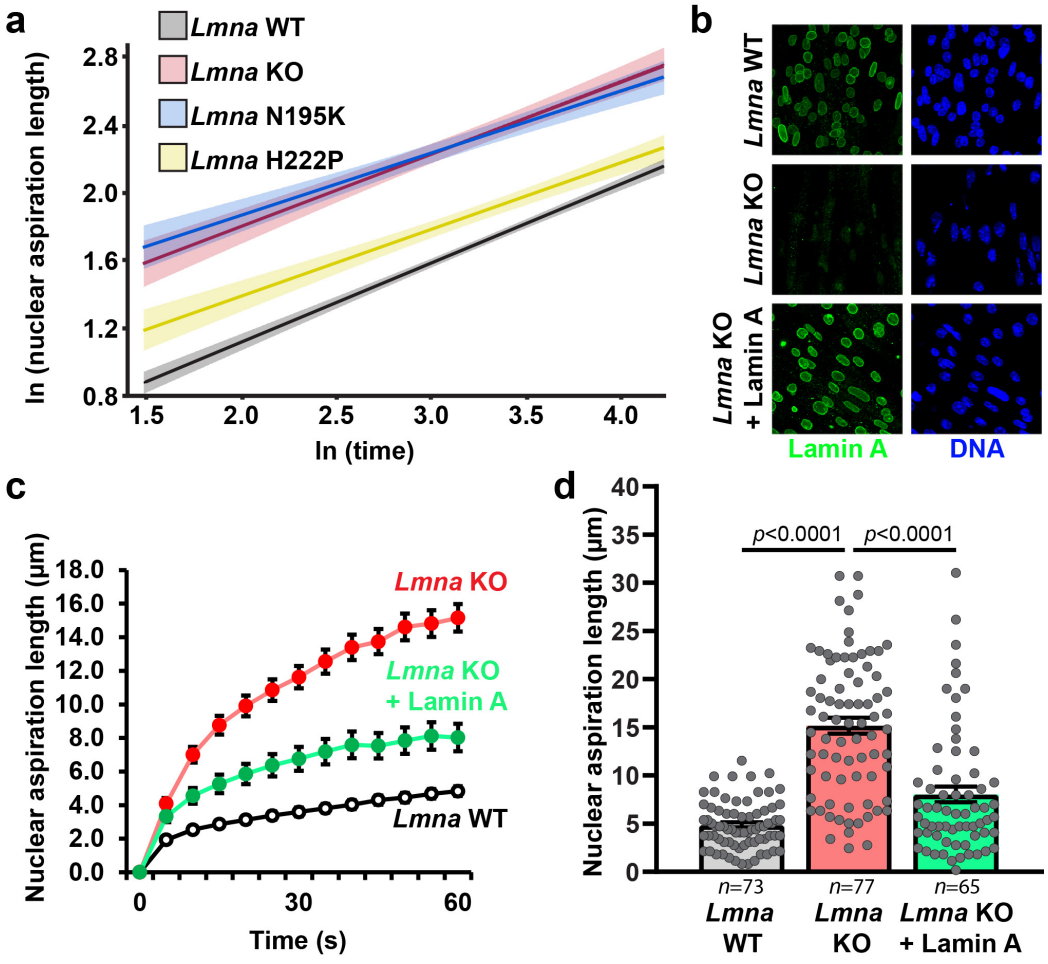

Supplementary Figure 3. **Micropipette aspiration analysis of *Lmna* mutant myoblasts and *Lmna* KO myoblasts ectopically expressing lamin A**. (**a**) Natural log transformation and plot of the micropipette aspiration data shown in Fig. 2b. The log-log data fits a two-tailed mixed-model linear regression model. A Dunnett-Hsu multiplicity corrected post-hoc analysis determined that all three *Lmna* mutants were significantly different ($p < 0.001$) from the wild-type controls. The slopes of the log-log data were not significantly different between the samples. A multilevel model including day-to-day variability confirmed that all three *Lmna* mutants were significantly different from the wild-type controls ($p < 0.0001$ for *Lmna* KO and *Lmna* N195K; $p < 0.001$ for *Lmna* H222P), although the statistical significance for the *Lmna* H222P myoblasts was lost when including additional variance components. $n = 233$, 57, 67, and 77 for *Lmna* WT, *Lmna* KO, *Lmna* N195K, and *Lmna* H222P, respectively. (**b**) Representative immunofluorescence images of lamin A expression in *Lmna* WT, *Lmna* KO and *Lmna* KO cells ectopically expressing lamin A (*Lmna* KO + lamin A). Experiment was repeated three times, with similar results (**c, d**) Measurement for nuclear deformation at 5 second intervals for *Lmna* WT, *Lmna* KO, and *Lmna* KO + Lamin A myoblasts during 60 seconds of aspiration (c), and quantification of the nuclear deformation after 60 seconds of aspiration (d), showing that ectopic expression of lamin A significantly improves nuclear stiffness in *Lmna* KO myoblasts. Data points are from *n* nuclei per genotype from three independent experiments. Significance determine by one-way ANOVA, using Tukey's correction for multiple comparisons. All bar plots show mean value ± standard error of the mean.

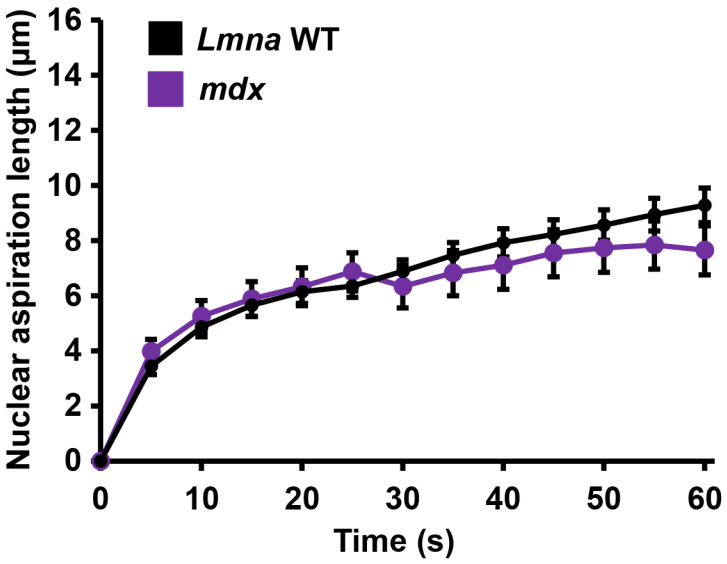

Supplementary Figure 4. *Mdx* myoblasts have normal nuclear stiffness. Measurement for nuclear deformation at 5 second intervals for *Lmna* WT and *mdx* myoblasts during 60 seconds of aspiration. $n = 35$ cells for *Lmna* WT and 67 cells for *Mdx* myoblasts. Line plots show mean value ± standard error of the mean.

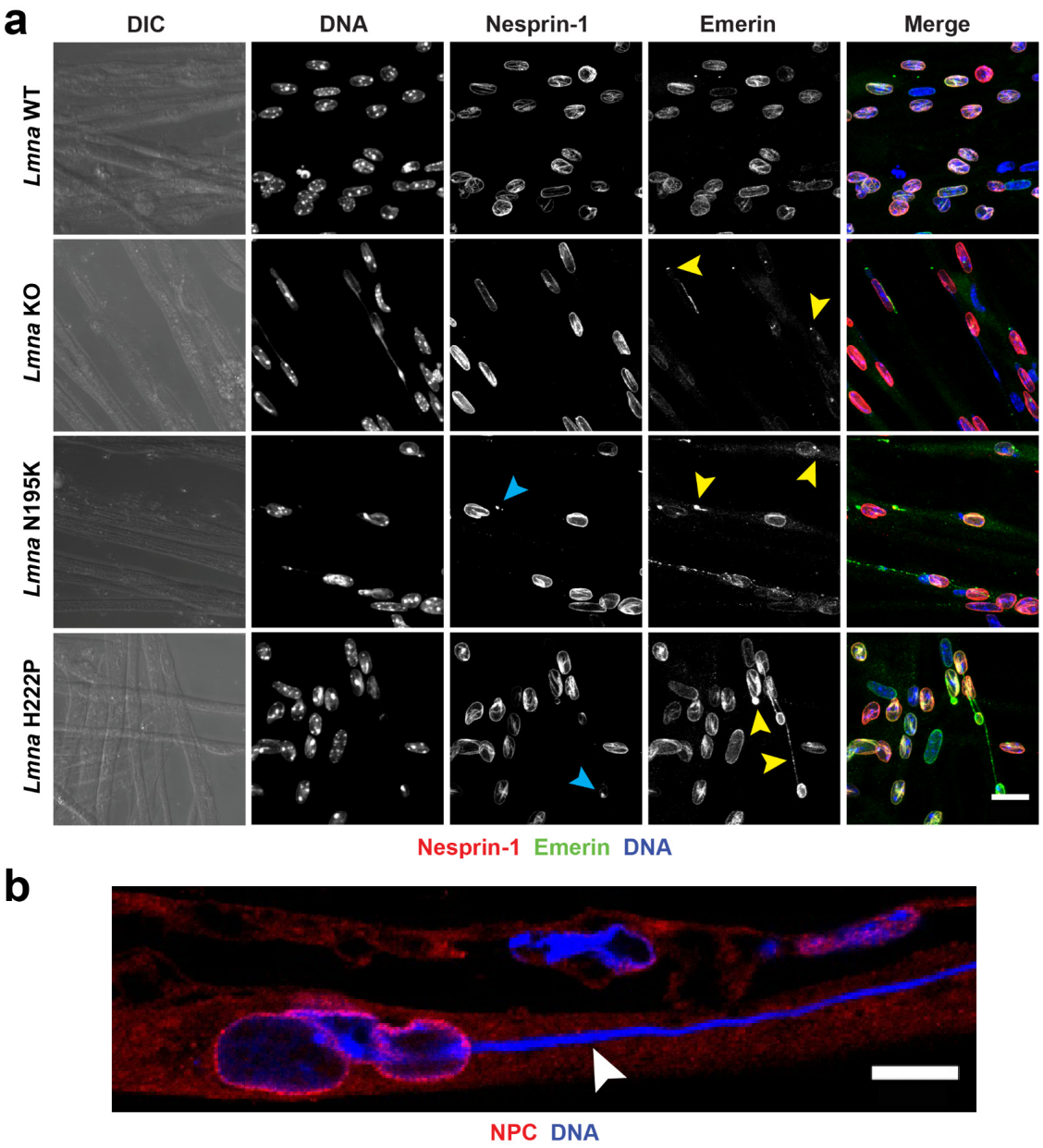

Supplementary Figure 5. Chromatin protrusions are surrounded by nuclear membranes containing emerin, with disturbed localization of nesprin-1 and nuclear pores. (**a**) Representative immunofluorescence images for nesprin-1 and emerin in *Lmna* WT, *Lmna* KO, *Lmna* N195K and *Lmna* H222P myofibers at day 5 of differentiation. Blue and yellow arrowheads denote chromatin protrusions that are enriched with nesprin-1 and emerin, respectively. Scale bar: 20 µm. The experiment was repeated three times with similar results. (**b**) Representative image of immunofluorescence detection of nuclear pore complexes (NPC) in *Lmna* KO myofibers at day 10 of differentiation, revealing absence of nuclear pores in the chromatin protrusion (arrowhead). Scale bar: 10 µm. The experiment was repeated three times with similar results.

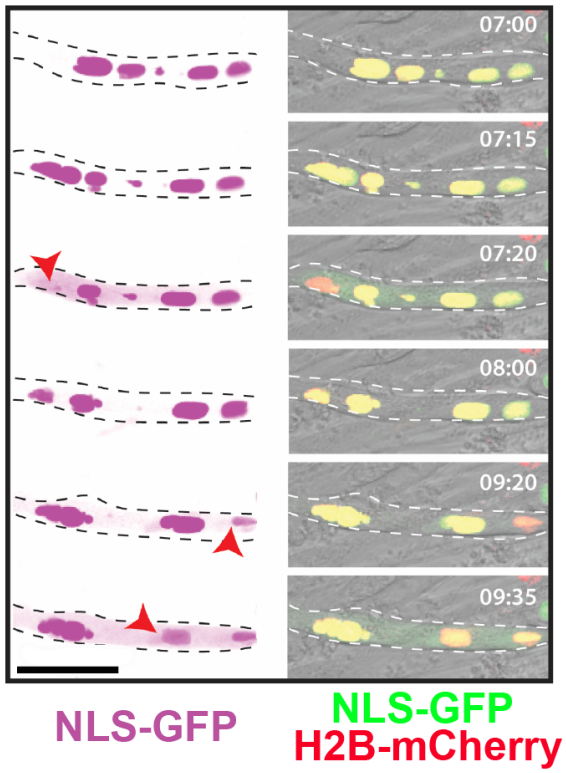

Supplementary Figure 6. *Lmna* mutant myonuclei undergo NE rupture *in vitro*. Representative time-lapse image sequence of NE rupture in *Lmna* KO myonuclei. Red arrowheads mark two nuclei that undergo NE rupture, visibly by transient loss of NLS-GFP from the nucleus. Scale bar: 50 µm for all images. Experiments were conducted a minimum of 3 times, with similar results in all experiments.

Supplementary Figure 7. Nuclear envelope rupture in *Lmna* KO muscle fibers is increased at myotendinous junctions. Representative image of a *Lmna* KO single isolated muscle fiber demonstrating the enrichment of cGAS+ nuclei at the myotendinous junctions (arrowheads). Scale bar: 200 µm. Similar results were observed in a minimum of 10 myofibers from multiple animals.

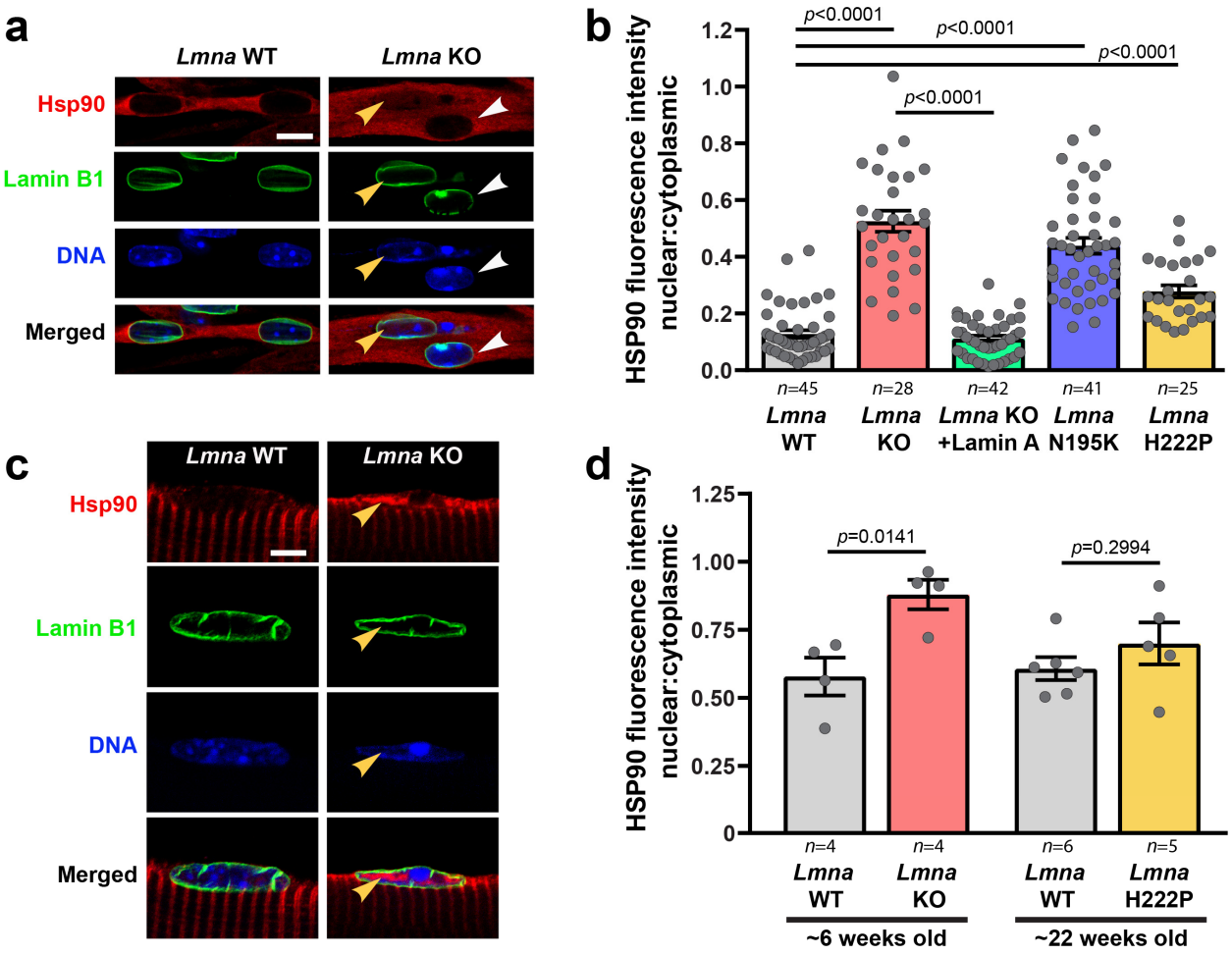

Supplementary Figure 8. *Lmna* mutant myonuclei have increased presence of Hsp90 *in vitro* and *in vivo*. (**a**) Representative image of nuclear localization of a large cytosolic protein, Hsp90, inside *Lmna* KO nuclei in myofiber differentiated for 10 days. White arrow indicates a nucleus with no observable chromatin defect and little Hsp90 nuclear accumulation, while the yellow arrow marks a nucleus with a chromatin protrusion and increased nuclear Hsp90 accumulation. Scale bar: 10 µm. (**b**) Quantification of the fluorescence intensity of nuclear Hsp90 levels for *Lmna* WT, *Lmna* KO, *Lmna* KO + Lamin A, *Lmna* N195K and *Lmna* H222P myofibers *in vitro*. For each nucleus, the nuclear fluorescence intensity was normalized to the cytosolic intensity immediately adjacent to each nucleus. Data based on *n* nuclei per genotype from three independent experiments. Significance determined by one-way ANOVA, using Tukey's correction for multiple comparisons. (**c**) Representative image of Hsp90 nuclear localization in myonuclei from *Lmna* WT and *Lmna* KO mice. Scale bar: 10 µm. (**d**) Quantification of the fluorescence intensity of nuclear Hsp90 levels for *Lmna* WT, *Lmna* KO, and *Lmna* H222P isolated single fibers. For each nucleus, the nuclear fluorescence intensity was normalized to the cytosolic intensity immediately beside each nucleus. Data based on *n* mice per genotype, with 13-16 nuclei quantified per animal. Significance determined by two-tailed students t-test within each genotype. All bar plots show mean value ± standard error of the mean.

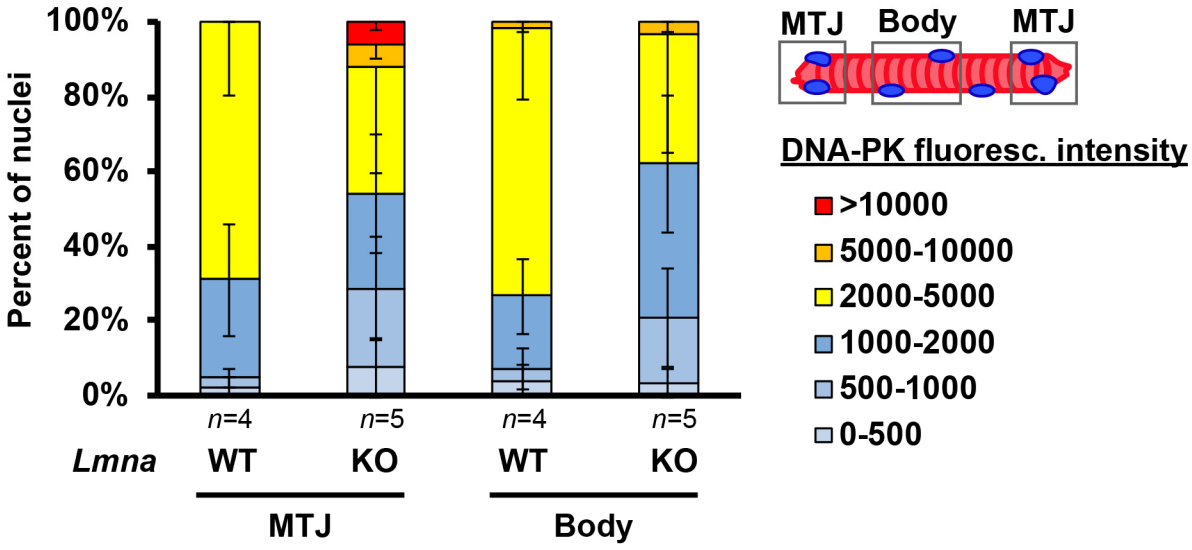

Supplementary Figure 9. *Lmna* KO MTJ myonuclei have increased DNA-PK activity *in vivo*. Quantification of p-DNA-PKcs immunofluorescence in isolated muscle fibers from *Lmna* and *Lmna* KO mice. Data based on *n* mice per genotype. All bar plots show mean value ± standard error of the mean.

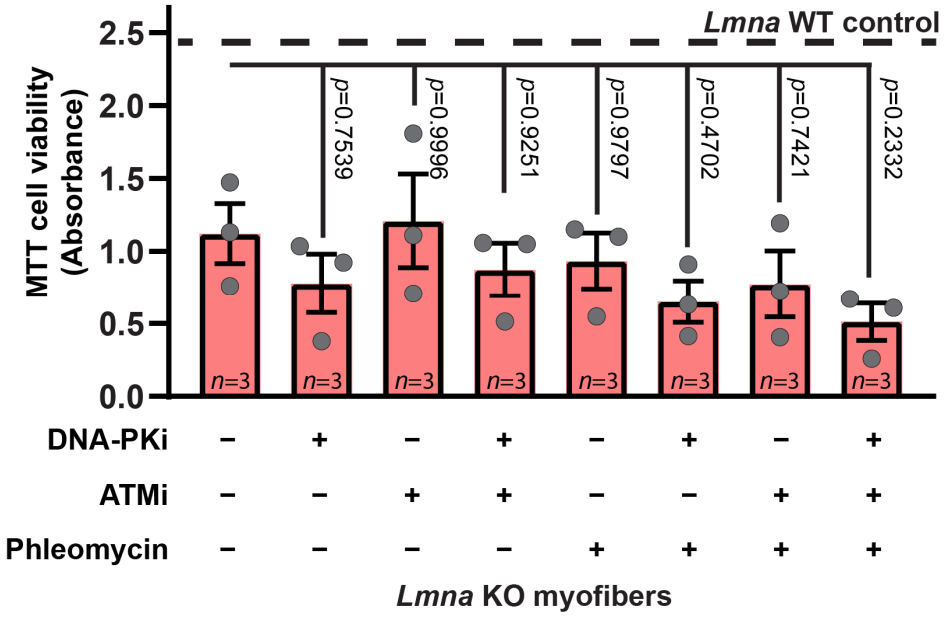

Supplementary Figure 10. Inducing DNA damage or inhibiting DNA repair does not promote additional cells death in *Lmna* KO myofibers. Quantification of cellular viability in *Lmna* KO myofibers using MTT assay following DNA damage induction with phleomycin, with and without concurrent treatment with inhibitors for DNA-PK (NU7441) and/or ATM (KU55933). Dashed line indicates corresponding values for *Lmna* WT control. Data based on *n* independent experiments per condition. All bar plots show mean value ± standard error of the mean.

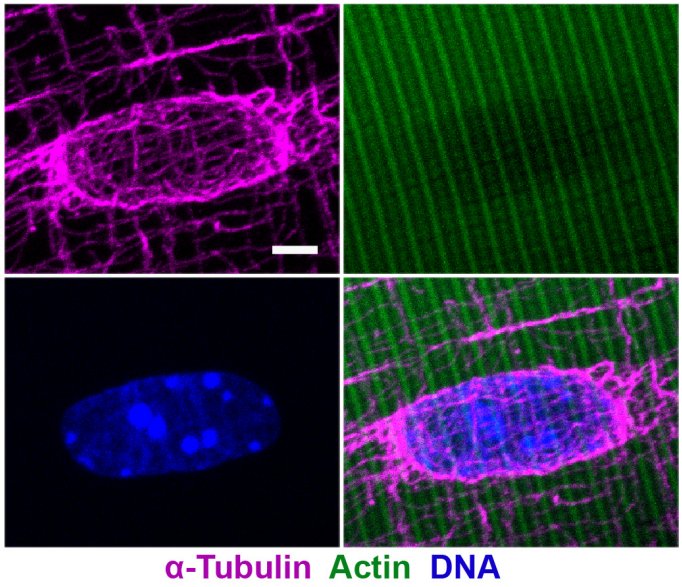

Supplementary Figure 11. Microtubules form cage-like structures around myonuclei. Representative immunofluorescence image of an isolated *Lmna* WT muscle fiber stained for tubulin (magenta), F-actin (green), and DNA (blue), showing characteristic 'microtubule cage' around myonucleus. Scale bar: 5 µm. Similar results were observed in minimum of 10 myofibers.

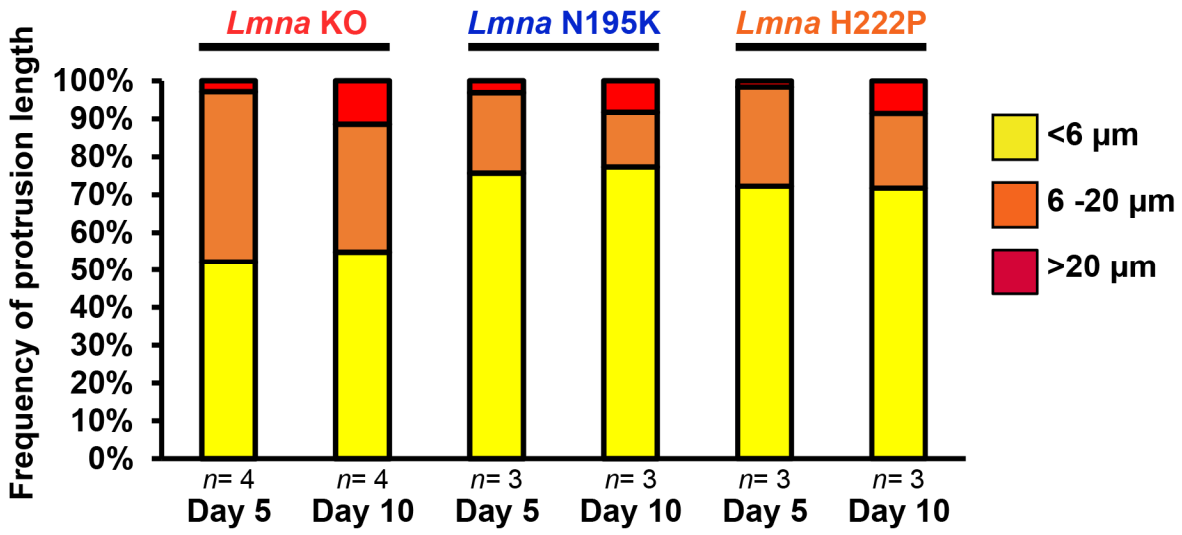

Supplementary Figure 12. Fraction of nuclei with severe chromatin protrusions increased over time in *Lmna* mutant myofibers. Quantification of the relative distribution of chromatin protrusion lengths in *Lmna* KO, *Lmna* N195K, and *Lmna* H222P muscle cells at day 5 and day 10 of *in vitro* differentiation. Data based on *n* independent cell lines per genotype.

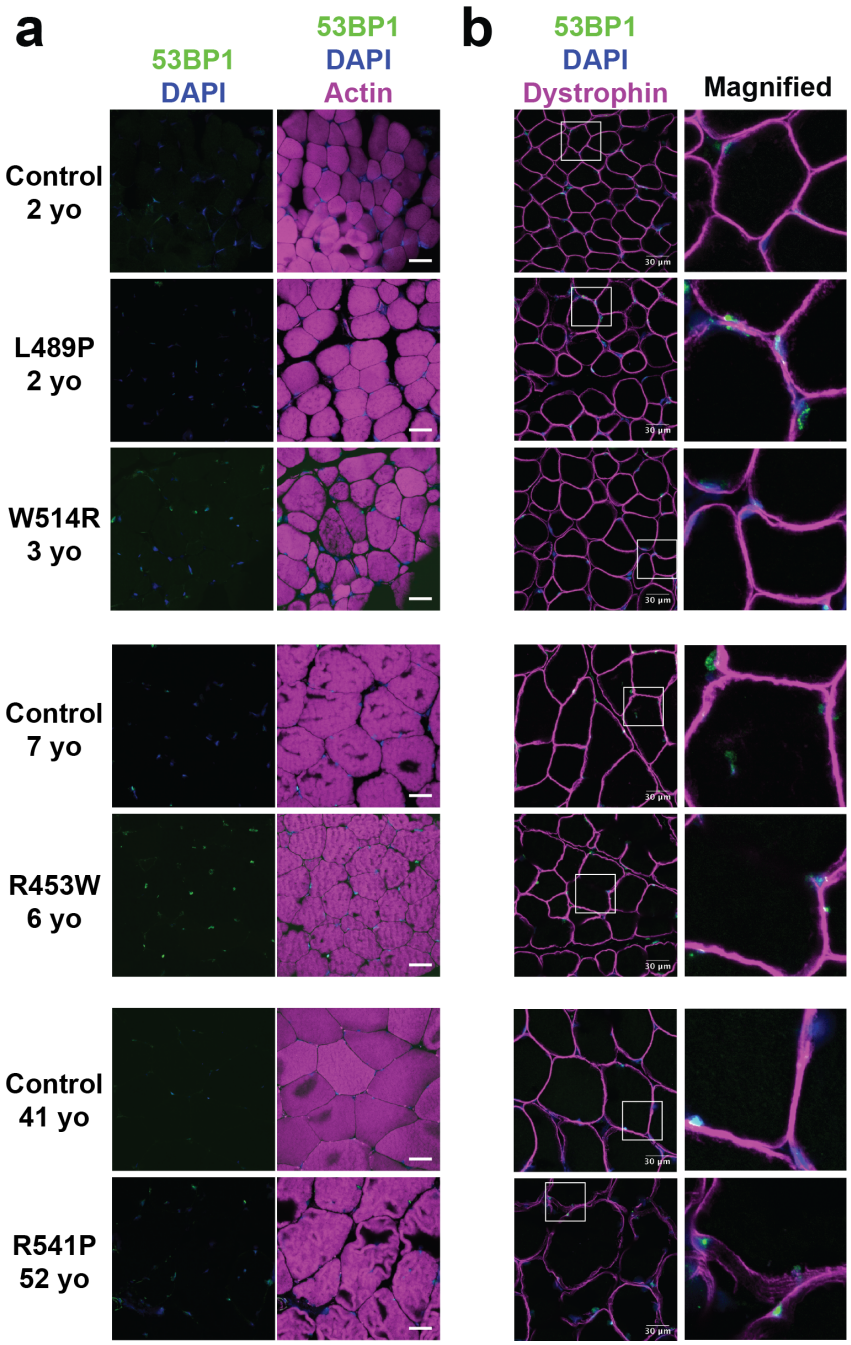

Supplementary Figure 13. Increased DNA damage in human laminopathy muscle tissue. Representative images of cryopreserved human muscle biopsy tissue from individuals with *LMNA*-related muscular dystrophy and age-matched controls, stained with antibodies to (a) 53BP1 or (b) 53BP1 and dystrophin, and additionally stained for DNA (DAPI) and F-actin (Phalloidin). Two to three independent experiments were performed for each genotype. At least four images were obtained from each tissue sample for each experiment, with similar results obtained among experiments. In panel b, the boxed regions in the left column are shown as close-up in the right column, revealing increased anti-53BP1 staining in muscle from laminopathy individuals versus age-matched controls.

SUPPLEMENTARY MOVIES

Supplementary Movies 1-4. Representative movies of spontaneous contractions in *Lmna* WT, *Lmna* KO, *Lmna* N195K, and *Lmna* H222P myofibers after 10 days of differentiation. Experiments were performed at least three independent times, with similar results (see Extended Data Fig. 1).

Supplementary Movie 5. Representative movie of micropipette aspiration of *Lmna* WT, *Lmna* KO *Lmna* N195K, and *Lmna* H222P myoblasts. Experiments were performed at least three independent times, in over 60 cells per genotype, with similar results (see Fig. 2C and Suppl. Fig. 3).

Supplementary Movie 6. Representative movie of microharpoon manipulation of *Lmna* WT and *Lmna* KO myotubes after day 5 of differentiation. Similar results were obtained in three independent experiments, using >10 nuclei per condition (see Fig. 2d,e).

Supplementary Movie 7. Time-lapse of nuclear envelope rupture in *Lmna* KO myotubes after four days of differentiation. Note the loss of soluble NLS-GFP from the nucleus into the cytoplasm. Similar results were obtained in at least three independent experiments.

Supplementary Movie 8. Representative movie of microharpoon manipulation of *Lmna* KO myotubes after day 5 of differentiation following 24 hours of treatment with either 50 nM paclitaxel or DMSO control. Similar results were obtained in three independent experiments, using >10 nuclei per condition (see Extended Data Fig. 6)

Supplementary Movie 9. Time-lapse of nuclear envelope rupture during myonuclear movement at 5 days of differentiation. Note the loss of NLS-GFP from the nucleus is immediately followed by the formation of cGAS-mCherry foci at the site of rupture. Experiments were conducted a minimum of three times, with similar results in all experiments.

Supplementary Movies 10-13. Representative movies of spontaneous contractions in *Lmna* WT myofibers after 10 days of differentiation expressing a doxycycline inducible GFP-KASH2 to disrupt nucleo-cytoskeletal force transmission or the GFP-KASH2ext control, and the corresponding non-doxycycline induced controls. Experiments were performed in six replicates in two independent experiments, with similar results (see Extended Data Fig. 9).

Supplementary Movies 14-17. Representative movies of spontaneous contractions in *Lmna KO* myofibers after 10 days of differentiation expressing a doxycycline inducible GFP-KASH2 to disrupt nucleo-cytoskeletal force transmission or the GFP-KASH2ext control, and the corresponding non-doxycycline induced controls. Experiments were performed in six replicates in two independent experiments, with similar results (see Extended Data Fig. 9).

SUPPLEMENTARY TABLES:

Nucleotide change	Amino acid substitution	Age on onset	Age of diagnosis (years)	Age when muscle biopsy obtained (years)	Tentative diagnosis/comments	Reference
745C>T	R249W	3 months	<1	1	Congenital MD, early onset with dropped head, unable to sit unassisted at age 3 years	unpublished
1346G>T	G449V	6 months	3	1	Congenital MD, non-ambulatory at age 13 years	[1, 2]
1466T>C	L489P	<2	7	2	Congenital MD , moderately severe at age 2 years	[1, 2]
1540T>C	W514R	2-3 yo	5	3	Mild to moderate myopathy at age 14 years	[1, 2]
1357C>T	R453W	n.a.	6	10	Mild myopathy at age 5.5 years	unpublished
1622G>C	R541P	n.a.	<52	52	n.a.	unpublished

Supplementary Table 1. Description of *LMNA* patients and muscle biopsy samples used for immunofluorescence analysis. n.a.; not available

Antibody	Cat#	Vendor	Dilution
MyHC	A4.1025	DSHB	1:100
MyHC	MAB4470-SP	Novus Biologicals	1:500
Lamin B (M-20)	sc-6217	Santa Cruz	1:200
Lamin B1 (B-10)	sc-374015	Santa Cruz	1:200
Lamin A (H-102)	sc-20680	Santa Cruz	1:200
Lamin A/C (E1)	sc-376248	Santa Cruz	1:200
Gamma-H2AX (Ser139)	80312	Cell Signaling	1:200
Gamma-H2AX (Ser139)	9718	Cell Signaling	1:200
HSP90 α/β (F-8)	sc-13119	Santa Cruz	1:200
Nesprin1-E	MANNES1E	Glen Morris	1:500
Nesprin-1-A	MANNES1A	Glen Morris	1:500
alpha-tubulin	T9026	Sigma	1:500 (IF) 1:5000 (WB)
NPC (414)	Ab50008	Abcam	1:500
Emerin	NCL-EMERIN	Leica	1:200
DNA-PKcs (S2056)	ab18192	Abcam	1:1000
DNA-PKcs	sc-390849	Santa Cruz	1:750
Cleaved Caspase-3	9661	Cell Signaling	1:500
53BP1	NB100-304	Novus Biologicals	1:1000
Alexa Fluor 488; Donkey anti-mouse	A-21202	Invitrogen	1:250
Alexa Fluor 568; Donkey anti-mouse	A10037	Invitrogen	1:250
Alexa Fluor 647; Donkey anti-mouse	A-31571	Invitrogen	1:250
Alexa Fluor 488; Donkey anti-rabbit	A-21206	Invitrogen	1:250
Alexa Fluor 568; Donkey anti-rabbit	A10042	Invitrogen	1:250
Alexa Fluor 647; Donkey anti-rabbit	A-31573	Invitrogen	1:250

IRDye® 800CW Donkey anti-Rabbit IgG	926-32213	Li-cor	1:2000
IRDye® 680RD Donkey anti-Mouse IgG	926-68072	Li-cor	1:3000

Supplementary Table 2. Antibodies and corresponding dilutions. Primary and secondary antibodies for immunofluorescence staining and western blotting.

REFERENCES

1. Dialynas, G. *et al.* LMNA variants cause cytoplasmic distribution of nuclear pore proteins in Drosophila and human muscle. *Hum Mol Genet* **21**, 1544-1556 (2012).
2. Dialynas, G. *et al.* Myopathic lamin mutations cause reductive stress and activate the nrf2/keap-1 pathway. *PLoS Genet* **11**, e1005231 (2015).